

TES HYPERSPECTRAL MAPPING OF PROPOSED PALEOLAKE BASINS IN THE AEOLIS QUADRANGLE OF MARS: A SEARCH FOR AQUEOUS MINERALS K. R. Stockstill¹, S. Ruff², J. E. Moersch¹, A. Baldrige², J. Farmer², ¹Dept. Geol. Sci., Univ. Tennessee, 306 G.S. Bldg., Knoxville, TN 37996, kstockst@utk.edu, ²Dept. Geol. Sci., Arizona State Univ., Tempe, AZ 85287.

Introduction: Several studies have presented geomorphic evidence that supports the existence of paleolake basins on Mars [1,2 and others]. A list of proposed paleolake basins in impact craters was compiled [1] and these workers noted that some basins displaying alternating bands of light and dark albedo materials conformal with the basin margins. They suggested that the bright materials may be evaporite deposits, but this has been debated [3]. Thus far, TES searches for aqueously derived minerals on a global scale have only detected coarse-grained crystalline hematite [4]. We are currently conducting a regional study to search for small exposures of evaporite minerals within putative paleolake basins on Mars. Detection of evaporites on Mars would provide constraints on its paleoclimate.

Method: The spectra for each target are assembled into a hyperspectral cube. Because we expect spectral features of evaporite minerals to be extremely subtle, we preserve individual unprocessed emissivity spectra as far into the processing chain as possible.

A principle component analysis (PCA) algorithm is run on the hyperspectral cubes. The resultant PCA images have some contiguous areas where similar PCA values span several orbits, which we interpret to represent real spectral units at the surface. In other instances, similar PCA values are confined to specific orbit tracks, which we interpret to represent inter-orbital atmospheric variations. We reject these orbits because we want to minimize atmospheric contributions to total spectral variance in the scene. These orbits are identified and the hyperspectral cubes are re-assembled from the original set of spectra minus these orbital tracks. This process is repeated until most of the color variations in the PCA images appear to be associated with spectral units on the ground. The final PCA images are used to define regions of interest (ROIs) that correspond to spectral units in the scenes. Averaged spectra from each ROI are extracted and examined to see what spectral features distinguish these units from each other.

The averaged region-of-interest spectra were first evaluated for the presence of dust/fine particulate materials based on their dust cover index (DCI) [5]. Next, a linear least squares deconvolution was applied using seven previously-reported and one new TES spectral endmembers: Acidalia and Syrtis Surface Types, hematite, two atmospheric dust endmembers and two

water ice cloud endmembers [6], plus a new surface dust endmember [7]. If an averaged spectrum had a DCI value below the threshold (0.96) for “dust free” and the deconvolution routine used the surface dust endmember, the spectrum was considered to represent a dusty surface. Because the spectral library we used [8] contains only coarse particulate samples, and because linear unmixing may not apply to fine particulate mixtures, no further analysis was performed on TES spectra not meeting the “dust-free” criterion. In addition, if the spectrum was well-modeled by linear unmixing using the eight previously-reported TES surface and atmospheric endmembers and no anomalies were detected by visual inspection, then further analyses were also considered unnecessary. Atmospheric correction was performed on the remaining region-of-interest spectra using the method described by [9].

The remaining atmospherically-corrected region-of-interest spectra were deconvolved twice using library spectra of individual minerals: once using the igneous minerals thought to be present in previously-reported TES surface spectra and once using these spectra plus library spectra of evaporite and hydrothermal minerals. If the spectral signatures of these aqueous minerals are not present in the region-of-interest spectra, the results of the igneous-only and igneous-plus-aqueous deconvolution runs should be approximately the same.

Results: Figure 1 shows an RGB composite image of the first three PCA bands- from a TES hyperspectral cube covering one of our target basins, Gale Crater (5.5S, 137.8E). Arrows point to orbits that were removed in subsequent re-assembly of the hyperspectral cube. Figure 2 displays the final PCA band color composite image by which ROIs were defined.

The central mound in Gale Crater, shown by the red region in Figure 2, had a DCI value of 0.93, below the threshold for a dust-free surface. In addition, the results of the deconvolution used the surface dust endmember (Table 1). This spectrum represents a typical dusty surface and was not processed further.

The southern portion of the basin floor, shown by blues in Figure 2, had a DCI value of 0.97, above the threshold for a dust-free surface. In addition, the deconvolution using the standard TES spectral endmembers did not choose the surface dust endmember (Table 2). Therefore, this spectrum represents a relatively dust-free surface. This spectrum was well-modeled

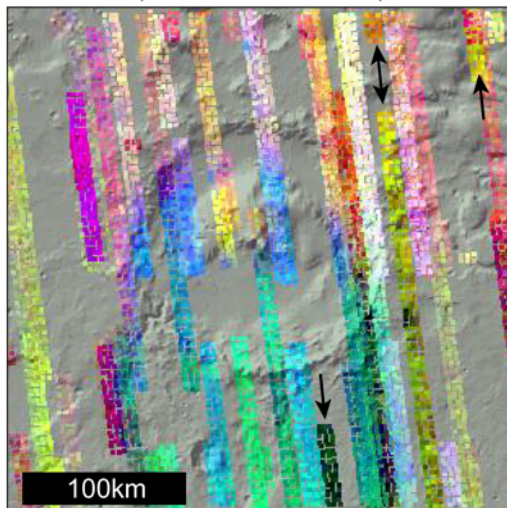
using just TES atmospheric and surface endmembers, (Syrtsis Type Surface), requiring no further processing.

The northern portion of the basin floor, shown by greens in Figure 2, had a DCI value of 0.95, just below the threshold for a dust-free surface. The deconvolution also used the surface dust endmember (Table 3). Our interpretation is that this surface may be a mixture of the previous two spectral classes, with enough surface dust to obviate further deconvolution.

Region-of-interest spectra of Gusev Crater (14.5 S, 175.5 E) were dominated by atmospheric endmembers and surface dust with DCI values below the threshold value. An unnamed crater located at (10.0 S, 144.5 E) had a combination of dusty and “dust-free” region-of-interest spectra. The “dust-free” spectra were well-modeled with a combination of previously-reported TES endmembers. Results of this method for additional candidate locations will be presented in the poster. Thus far, no aqueous minerals have been detected in any basins with the Aeolis Quadrangle.

References: [1] Cabrol N. and Grin E. (2000) *Icarus*, 149, pp. 291-328. [2] Forsythe R. and Zimbelman J. (1995) *JGR*, 100, 5553-5563. [3] Ruff S. et al. (2001) *JGR*, 106, 23921-23927. [4] Christensen P. et al. (2000) *JGR*, 105, 9623-9642. [5] Ruff S. and Christensen P. (2002) *JGR*, 107, 5127-5149. [6] Bandfield J. et al. (2000) *JGR*, 105, 9573-9587. [7] Bandfield J. and Smith M. (2003) submitted to *Icarus*. [8] Christensen P. et al. (2000) *JGR*, 105, 9735-9738. [9] Smith M. et al. (2000), *JGR*, 105, 9589-9607.

(2.9S, 135.2E) (2.9S, 140.4E)



(8.1S, 135.2E) (8.1S, 140.4E)

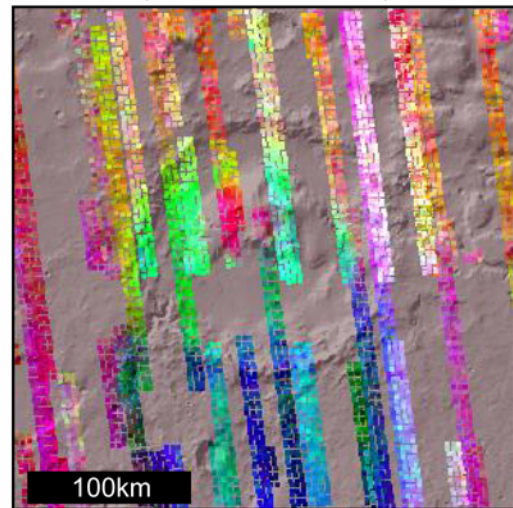
Figure 1: First three PCA bands displayed as a color composite for Gale Crater. Arrows indicate orbits that were removed in subsequent processing steps because the contribution of atmospheric components in these orbits deviated slightly from the scene mean.

| Table 1: Model derived modes for mean spectrum of the Basin Center. | | DCI value 0.93 |
|--|--|-------------------|
| Acidalia type surface | | 8.0 |
| Dust Low CO2 | | 33.2 |
| Dust High CO2 | | 16.0 |
| Water Ice Cloud2 | | 9.2 |
| Surface Dust | | 34.6 |
| Total | | 101.0 |

| Table 2: Model derived modes for mean spectrum of the S. Basin Floor. | | DCI value 0.97 |
|--|--|-------------------|
| Syrtsis type surface | | 35.2 |
| Dust Low CO2 | | 60.0 |
| Water Ice Cloud2 | | 3.7 |
| Total | | 98.9 |

| Table 3: Model derived modes for mean spectrum of the N. Basin Floor. | | DCI value 0.95 |
|--|--|-------------------|
| Syrtsis type surface | | 1.3 |
| Dust Low CO2 | | 65.1 |
| Dust High CO2 | | 2.9 |
| Water Ice Cloud2 | | 7.8 |
| Surface Dust | | 22.9 |
| Total | | 99.9 |

(2.9S, 135.2E) (2.9S, 140.4E)



(8.1S, 135.2E) (8.1S, 140.4E)

Figure 2: Final PC image, displayed as in Figure 1, from which ROIs were defined from contiguous regions of color. The central mound is clearly visible in red tones near the center of the basin. Two additional regions of interest were defined by the northern green and southern blue regions within the basin floor.